

# TECHNICAL RESEARCH REPORT

## I-Q TCM: Reliable Communication Over the Rayleigh Fading Channel Close to the Cutoff Rate

*by S.A. Al-Semari, T. E. Fuja*

**T.R. 96-45**



*Sponsored by  
the National Science Foundation  
Engineering Research Center Program,  
the University of Maryland,  
Harvard University,  
and Industry*

# I-Q TCM: Reliable Communication Over the Rayleigh Fading Channel Close to the Cutoff Rate

Saud A. Al-Semari and Thomas E. Fuja \*

Department of Electrical Engineering

Institute for Systems Research

University of Maryland

College Park, MD 20742

May 17, 1996

## Abstract

This paper presents some trellis codes that provide high coding gain over the frequency non-selective slowly Rayleigh distributed fading channel. It is shown that the use of two encoders in parallel – used to specify the in-phase and quadrature components of the transmitted signal – results in greater minimum time diversity than the conventional design in which a single encoder is used. Using this approach – which we label “I-Q TCM” – codes with bandwidth efficiencies of 1,2, and 3 bits/sec/Hz are described for various constraint lengths. The performance of these codes is bounded analytically and approximated via simulation; the results show a large improvement in the BER when compared with conventional TCM schemes when perfect channel state information (CSI) is available to the receiver. Indeed, when this approach is applied to channels with independent Rayleigh fading, the resulting coding gain is close to that implied by the cutoff rate limit, even for only moderately complex systems.

The proposed codes are also simulated under less ideal assumptions. For instance, results for a 1 bit/sec/Hz IQ-TCM code *without* CSI show a significant gain over conventional coding. Finally, simulations over channels with correlated fading were undertaken; it is concluded that an interleaver span of  $4\nu$  yields performance close to what is achieved with ideal interleaving.

Submitted June 1995 to IEEE Transactions on Information Theory

Revised April 1996

**Index Terms:** Trellis-coded modulation, Rayleigh fading channels, correlated fading, interleaving, land-mobile radio channels, minimum time diversity, I-Q TCM.

---

\*This research was supported in part by National Science Foundation grant NCR-8957623; also by the NSF Engineering Research Centers Program, CDR-8803012.

# 1 Introduction

In cellular mobile radio channels, the transmitted signal typically suffers distortion from fading. One of the most commonly assumed models is that of a frequency non-selective slowly Rayleigh distributed fading channel; this model has been used to characterize the channel behavior of mobile radio systems [1]-[4]. The effect of fading is a substantial degradation of the system error rate performance.

Diversity is a popular method for mitigating the effects of fading. One of its simplest forms is time diversity, in which each symbol is repeated in  $L$  different time slots such that the slots are affected by independent fades. This approach – called  $L$ -fold time diversity – can be viewed as an  $(L, 1)$  repetition code with a minimum Hamming distance of  $L$ . Therefore, it may be expected that more sophisticated block or convolutional codes with large minimum Hamming distance could yield significant gains over uncoded systems.

However, channel coding raises the possibility of bandwidth expansion; in bandlimited environments, such expansion might not be acceptable. Ungerboeck [5] stimulated most of the research in bandwidth-efficient coding with his introduction of trellis coded modulation (TCM). While originally applied to AWGN channels, the use of TCM for fading channels has received considerable attention in recent years.

## 1.1 Relevant Past Work

Divsalar and Simon [6]-[8] were the first to evaluate the performance of trellis coded modulation for Rayleigh/Rician channels. They showed that substantial performance improvement can be achieved using simple TCM schemes combined with interleaving; the interleaving can be viewed as a zero redundancy code that “randomizes” the distribution of the errors, breaking up bursts and destroying the memory of the channel. Interleaving may be used in conjunction with a scheme for extracting state information – i.e., the attenuation of the fade – to recover some of the channel capacity lost due to the interleaving.

Divsalar and Simon [6] also derived Chernoff upper bounds on the pairwise error proba-

bility. They pointed out that the effective minimum time diversity of the code is equivalent to its minimum Hamming distance (in signal symbols); moreover, the performance of a code over the Rayleigh-distributed fading channel depends strongly on the code's minimum time diversity and very weakly on its minimum squared Euclidean distance – the most important performance parameter for non-fading AWGN channels. This means that trellis codes that are optimal for non-fading AWGN channels are, except for a few cases, sub-optimal for fading channels. An exact characterization of the pairwise error-probability in the Rayleigh fading environment was given in [9] and [10].

A number of papers dealing with the optimization of TCM codes for the Rayleigh channel have appeared [11]-[14]. Most of these coding schemes use the traditional Ungerboeck approach in their design – i.e., they involve doubling the constellation size over what is required for uncoded transmission and the use of a rate  $k/(k+1)$  encoder to describe valid symbol sequences. However, if a rate  $k/(k+1)$  code is used, the achievable minimum time diversity  $L$  is upper bounded by  $L \leq \lfloor \nu/k \rfloor + 1$ , where  $\nu$  is the number of memory elements in the encoder. Therefore, the larger the number of the encoder input bits, the more memory elements are needed for a given minimum time diversity. This suggests that if the input bits are distributed to different convolutional encoders, the minimum time diversity could be increased. This is one motivation behind using multilevel codes for the Rayleigh channel [15]-[17]. However, multilevel codes with multistage decoding require a large delay at the decoder to get near-optimal performance.

The problem of transmitting two bits/symbol over the Rayleigh channel with 8-PSK modulation was considered by Zehavi [19]; he showed that using three bit interleavers can provide additional coding gain. The use of multidimensional trellis codes for the Rayleigh fading channel was investigated in [20] and [21]. Multidimensional TCM permits the design of systems with non-integer bandwidth efficiencies and improves the error performance for low constraint length codes. However, a disadvantage of multidimensional TCM is the increased number of input bits to the encoder, which limits the minimum time diversity of the code.

Also, more interleaving and a larger decoder buffer are needed; this increases the delay, which may prohibit the use of such codes in real-time applications.

All of the results described above fall far short of the performance promised by  $R_0$ , the computational cutoff rate limit. For example, for 8-PSK TCM schemes with two information bits per baud over a channel with independent Rayleigh fading, cutoff rate curves show that reliable communication can be achieved at  $E_b/N_o = 9$  dB, while the best code currently known requires  $E_b/N_o = 14.5$  dB to provide a BER of  $10^{-5}$  [19].

## 1.2 Proposed Codes

To achieve a larger minimum time diversity, we propose distributing the data bits to two parallel encoders; the first encoder encodes the in-phase component of the signal while the second encodes the quadrature component. (See Figure 1.) This approach requires only two encoders/decoders and permits the two decoders to work independently; by comparison, multilevel codes typically require more than two encoders/decoders and incur substantial delay to approach optimal performance. In this paper, examples of codes with bandwidth efficiencies of 1, 2, and 3 bits/sec/Hz and different constraint lengths are described. Their minimum time diversities are shown to be greater than that of the corresponding conventionally designed codes with the same complexity.

The idea of I-Q TCM first appeared in the “pragmatic” TCM design of Viterbi *et. al.* in which they used two off-the-shelf rate 1/2 64-state encoders to encode the in-phase and quadrature components of a QAM constellation [22]. This approach results in quadrupling the QAM constellation over what is required for uncoded transmission. Another approach that uses off-the-shelf convolutional codes with QAM modulation was suggested by Heegard, Lery, and Paik; in [23] they demonstrated how coded QAM modulation can be implemented using QPSK-based coded modulation, eliminating the need to quadruple the constellation.

Moher and Lodge [24] used the I-Q approach for transmitting 2 bits/sec/Hz on a satellite channel modeled with a Rician distribution; they showed that pilot symbol aided techniques

could effectively extract channel state information. Ho, Cavers, and Varaldi [25] used the I-Q approach to compare the performance of a single 8-state octal PSK trellis code with that of two parallel 4-state encoders – the latter resulting in 16-QAM signaling; they show that a large coding gain over the Rayleigh distributed channel is achieved, even if the ratio of peak-to-average power is deducted from the coding gain. However, no codes were given for a higher number of states or for different bandwidth efficiencies.

Our work here is a generalization of this idea. Systems with a throughput of 1, 2, and 3 bits/sec/Hz and different constraint lengths are described and compared to their corresponding conventional codes. If the throughput is not an even number; then the encoder is operated every two signaling intervals and thus produces 4-dimensional coded signals. Quadrupling the signal constellation is only required for the 2 bits/sec/Hz system.

The following section gives a summary of the channel model, the performance criterion, upper bounds on the bit error rate, and the coding gain limits drawn from the cutoff rate curves. Then, a description of the codes, their analytical and simulated performance over the ideal Rayleigh channel, and complexity comparisons are presented. Performance results for systems with finite interleaving on a cellular mobile correlated fading model are given in Section 4. Finally, Section 5 presents the conclusions.

## 2 Background

In this section we briefly review the problem of coded modulation over fading channels.

### 2.1 Channel Model and Performance Criterion

Let  $x_i$  be the complex signal input to the channel at time  $i$ . The channel introduces two kinds of distortion – multiplicative and additive. The received signal at time  $i$  is given by

$$y_i = \rho_i x_i + n_i$$

where  $\rho_i$  is a Rayleigh distributed random variable with  $E(\rho_i^2) = 1$ , and  $n_i$  is two dimensional additive white Gaussian noise with single sided power spectral density  $N_0$ . We assume that

the effect of fading on the transmitted signal phase is completely compensated for by the synchronization circuitry – i.e., perfect coherent detection is assumed.

The trellis encoder produces a sequence of signals  $\mathbf{x}_N = (x_1, x_2, \dots, x_N)$  that are transmitted over the fading channel. At the receiver, the received sequence  $\mathbf{y}_N = (y_1, y_2, \dots, y_N)$  is observed; furthermore, we assume that the fading amplitudes  $\rho_N = (\rho_1, \rho_2, \dots, \rho_N)$  can be perfectly recovered at the receiver. (This channel state information can be extracted using a variety of methods; see [26]-[28] for details.) The decoder then performs maximum likelihood (ML) decoding using the Viterbi algorithm and decoding metric

$$m(\mathbf{y}_N, \mathbf{x}_N; \rho_N) = \sum_{l=1}^N \ln P(y_l | x_l, \rho_l) \quad (1)$$

which can be simplified (up to multiplication by a constant) as

$$m(\mathbf{y}_N, \mathbf{x}_N; \rho_N) = - \sum_{l=1}^N |y_l - \rho_l x_l|^2 \quad (2)$$

The pairwise error probability  $P(\mathbf{x}_N, \hat{\mathbf{x}}_N)$  is the probability that the decoder chooses as its estimate the sequence  $\hat{\mathbf{x}}_N = (\hat{x}_1, \hat{x}_2, \dots, \hat{x}_N)$  when the transmitted sequence was in fact  $\mathbf{x}_N = (x_1, x_2, \dots, x_N)$ . This occurs if

$$\sum_{l=1}^N |y_l - \rho_l \hat{x}_l|^2 < \sum_{l=1}^N |y_l - \rho_l x_l|^2 \quad (3)$$

If the fading amplitudes  $\{\rho_l\}$  are independent – i.e., the channel is *fully interleaved* – then a bound on the pairwise error probability can be obtained as in [6]:

$$P(\mathbf{x}_N, \hat{\mathbf{x}}_N) \leq \prod_{l \in \eta} \frac{1}{1 + \frac{1}{4N_o} |x_l - \hat{x}_l|^2} \quad (4)$$

where  $\eta$  is the set of all  $l$  for which  $x_l \neq \hat{x}_l$ .

From (4), it's clear that the pairwise error probability is affected primarily by the symbol-wise Hamming distance between the code sequences; so the error event probability will be dominated by the minimum symbol-wise Hamming distance of the code – its *minimum time diversity*. A parameter of secondary importance is the minimum product distance among code sequences.

Generally, the error performance of a trellis code is computed via the generalized transfer function of the (pairwise) super-state diagram [29]. This diagram has  $2^{2\nu}$  states, where  $\nu$  is the number of memory elements in the encoder; thus this approach is impractical even for codes with few states. However, the codes presented here satisfy the quasi-regularity property of Zehavi and Wolf [30], allowing the use of the transfer function of a modified state diagram with only  $2^\nu$  states. To describe this modification, define the weight profile function

$$F(B_i, e, D) = \sum_d A_d D^{\rho^2 d^2 [s(c), s(c \oplus e)]} \quad i = 1, 2. \quad (5)$$

Here,  $B_1$  and  $B_2$  are the subsets forming the first-level partition of the signal constellation,  $e$  is a binary error vector,  $s(c)$  is the signal label corresponding to the binary encoder output vector  $c$ ,  $A_d$  is the number of signals with  $d^2[s(c), s(c \oplus e)] = d$  and  $\rho$  is the fading attenuation. (For codes satisfying the Zehavi-Wolf condition,  $F(B_1, e, D) = F(B_2, e, D)$ .)

Having defined the weight profile function, the branches in the state diagram are labeled with

$$\frac{I^r \bar{F}(B_1, \tilde{e}, D)}{2^k} \Big|_{D=\exp(-\frac{E_s}{4N_o})}$$

where  $\tilde{e}$  is the label of the signal relative to a transition,  $r$  is the number of input ‘‘ones’’ associated with  $\tilde{e}$ ,  $k$  is the number of input bits entering the encoder,  $E_s$  is the average signal energy, and the overbar denotes averaging over the fading distribution.

The bit error probability of the TCM system can be tightly upper bounded [31] by

$$P_b \leq \frac{1}{k} \left[ \frac{1}{2^{2L}} \sum_{j=1}^L \binom{2L-j-1}{L-1} \left( \frac{2}{1+x_{min}} \right)^j \right] \frac{\partial}{\partial I} T(D, I) \Big|_{I=1} \quad (6)$$

where  $L$  is the minimum time diversity of the code,  $T(D, I)$  is the code transfer function and

$$x_{min} = \sqrt{\frac{d_x^2/4N_o}{1+d_x^2/4N_o}} \quad (7)$$

$$d_x^2 = \min\{|x_i - x_j|^2, x_i \neq x_j\}$$



## 2.2 Cutoff Rate

Schlegel and Costello [13] showed that the cutoff rate of the fully interleaved Rayleigh fading channel is given by

$$R_0 = -\log_2 \min_{\lambda} \sum_{i=1}^A \sum_{j=1}^A P(x_i)P(x_j)C(x_i, x_j, \lambda) \text{ bits/transmitted signal.} \quad (8)$$

Here,  $P(x_j)$  is the probability of transmitting  $x_j$ ,  $A$  is the cardinality of the signal set,  $C(x_i, x_j, \lambda)$  is the Chernoff factor of  $x_i$  and  $x_j$ , and  $\lambda$  is the Chernoff parameter. Typically the signals are assumed to be equiprobable; moreover, in the case of ideal channel state information, an optimal value of  $\lambda$  is found and the Chernoff factor can be simplified to

$$C(x_i, x_j) = \frac{1}{1 + \frac{|x_i - x_j|^2}{4N_o}}. \quad (9)$$

Cutoff rate curves, in Figure 2, show that a significant coding gain can be achieved with a larger signal constellation. Specifically, if a system with two information bits per transmitted signal is to be designed, the traditional approach is to design a rate 2/3 convolutional encoder jointly with 8-PSK signal constellation. The cutoff rate limit for such scheme is  $E_b/N_o = 9$  dB. On the other hand, if 16-QAM is used the cutoff rate limit is reduced to  $E_b/N_o = 8$  dB.

## 3 The Structure of I-Q Trellis Coded Modulation

Recall the structure of the proposed system in Figure 1. The basic idea is to use two independent encoders in parallel to select the in-phase and quadrature components of the transmitted signal. Moreover, two independent decoders are used to recover the data associated with the in-phase and quadrature components of the received signal. Hence, this coding scheme is called I-Q TCM.

As an example, suppose we use two rate 1/2 encoders, with the outputs of each mapped to a 4-AM signal set. The resulting is a 16-QAM constellation for transmitting 2 bits/sec/Hz. This code structure appears in [25], where it is shown that a 4-state code thus designed has

a minimum time diversity of three, while the best 8-state/8-PSK code with a throughput of 2 bits/sec/Hz has a minimum time diversity of two.

Regarding the complexity of the proposed structure: Similar to [29], we measure complexity by the total number of non-parallel paths leaving all the states divided by the number of information bits associated with a transition through the trellis\*. Consider a conventional TCM scheme in which  $k = k_1 + k_2$  data bits enter the encoder every signaling interval, causing a transition; here,  $k_1$  is the number of “encoded” bits and  $k_2$  is the number of “uncoded” bits – i.e., there are  $2^{k_1}$  non-parallel “bundles” of  $2^{k_2}$  parallel paths leaving each state. If the encoder has  $\nu$  memory elements, the complexity is  $2^{\nu+k_1}/k$ .

By comparison, consider the following I-Q TCM schemes:

- If  $k$  is even, we split up the  $k$  data bits into two blocks of  $k/2$ , and use two  $k/2$ -input encoders every signaling interval to encode the in-phase and quadrature components of the transmitted signal; assume  $k_1/2$  of the  $k/2$  bits are “encoded” and  $k_2/2$  are “uncoded”. If each of the two encoders has  $\nu$  memory elements, then there are (in both encoders combined)  $2^{\nu+1}$  states with  $2^{k_1/2}$  non-parallel edges emanating from each state – thus a complexity of  $2^{\nu+1+(k_1/2)}/k$ .
- If  $k$  is odd we use two  $k$ -input encoders every *two* signaling intervals; assuming  $k_1$  of the  $k$  bits are “encoded”, the result is  $2^{\nu+1}$  states with  $2^{k_1}$  non-parallel edges emanating from each state to encode  $2k$  data bits – or a complexity of  $2^{\nu+1+k_1}/2k = 2^{\nu+k_1}/k$ .

It is clear, then, that using two encoders – each with  $\nu$  memory elements – to implement I-Q TCM is no more complex than using a single encoder with  $\nu$  memory elements at the same throughput.

The proposed codes are detailed in the following sections.

---

\* In [29] the complexity is normalized per transmitted two-dimensional signal; we opt here to normalize per information bit.

### 3.1 I-Q QPSK

To transmit 1 bit/sec/Hz, each of the two encoders must encode 0.5 bit/sec/Hz. Hence, each encoder will be rate 1/2 and will operate every two signaling intervals; furthermore, each of the two encoded bits coming out of an encoder will be mapped to a 2-AM signal. The output of the first encoder specifies the in-phase components of two consecutive signals, while the output of the second encoder specifies the quadrature components; thus two QPSK signals are generated every two signaling intervals. This approach dictates the use of convolutional codes optimized in terms of minimum Hamming distance [32]. Table 1 shows the generator polynomials and the minimum Hamming distances of the codes thus used. Figure 3 shows the trellis diagram of the 8-state code, and Figure 4 shows the BER of each code – both the analytical upper bound from equation (6) and error rates obtained via simulation. Note that, for the 64 state code, a BER of  $10^{-5}$  can be achieved at  $E_b/N_o = 7.5$  dB, while the cutoff rate limit is 5.5 dB. For this code the complexity is equivalent to that of a Gray mapped QPSK encoded system with 64 states.

### 3.2 I-Q 16-QAM

To transmit 2 bits/sec/Hz, two rate 1/2 encoders are used each signaling interval, with the output of each mapped to a 4-AM signal set; the result is a 16-QAM signal selected every signaling period. Gray mapping between the output bits of each encoder and the 4-AM signal set allows the use of convolutional codes optimized for Hamming distance; once again, the codes in Table 1 are used. With this approach, the minimum time diversity is bounded by  $L \leq \nu + 1$ , where  $\nu$  is the number of memory elements in each of the two encoders. By comparison, conventional 8-PSK codes sending two bits per baud have a minimum time diversity at most  $\lfloor \nu/2 \rfloor + 1$ . Figure 5 shows the trellis diagram of the 8-state code with  $L = 4$ .

Since the I and Q channels operate independently, the bit error performance for I-Q 16-QAM is identical to that of 4-AM. Figure 6 shows the BER performance for the different

codes. Note that a BER of  $10^{-5}$  can be achieved at  $E_b/N_o = 10.5$  dB using the 64-state code; this is close to the cutoff rate limit of 8 dB for 16-QAM signaling when 2 bits/sec/Hz are transmitted.

### 3.3 4D I-Q 16-QAM

To transmit 3 bits/sec/Hz, two rate 3/4 encoders are used every two signaling intervals. The four bits from each encoder select a pair of 4-AM signals; the output of the first encoder specifies the in-phase components of two consecutive signals, while the output of the second encoder specifies the quadrature components. Thus two 16-QAM signals are generated every two signaling intervals. Figure 7 shows the signal partitioning of the 4-AM signal set; this partitioning maximizes the symbol Hamming distance and the minimum squared product distance. An eight state code's trellis diagram is shown in Figure 8. For this code the minimum time diversity is two and the minimum squared product distance (MSPD) is  $16(\Delta_0^2)^2$  where  $\Delta_0$  is the spacing between the signal symbols in the 16-QAM signal set. Figure 9 shows the trellis diagram of a 16-state code, and Figure 10 shows the performance of these two codes. No codes with higher number of states are designed because of their large complexity and the small gain in performance due to the limited minimum time diversity.

### 3.4 Comparisons

Table 2 compares the time diversities of the proposed codes with those of conventionally-designed TCM schemes.

- The 1 bit/sec/Hz I-Q QPSK system is compared with conventional Gray-mapped QPSK used with a rate 1/2 convolutional code.
- The 2 bits/sec/Hz I-Q 16-QAM system is compared with TCM schemes based on 8-PSK designed by Schlegel and Costello [13].
- The 3 bits/sec/Hz four-dimensional I-Q 16-QAM system is compared with codes employing 16-QAM signaling proposed by Du and Vucetic [14].

In each case a comparison is made between two codes of the same complexity, and in each case the I-Q code has a substantially higher minimum time diversity than the conventional TCM scheme. (The only exception: An eight-state 3 bits/sec/Hz code from [14] is compared with an eight-state 3 bits/sec/Hz I-Q TCM code; the time diversities are identical, but the complexity of the I-Q TCM code is one-half that of the code from [14]. In addition, the MSPD of the I-Q TCM code is  $16(\Delta_0^2)^2$  while the MSPD of the code from [14] is  $5(\Delta_0^2)^2$ .)

Figures 11-13 show the results of simulations that compare the I-Q TCM codes with conventional codes. The coding gains at a BER of  $10^{-5}$  range from 2 dB (for I-Q QPSK) to more than 5 dB (for 4D I-Q 16-QAM).

Two final points about the comparisons:

- While we generally compared codes of the same *complexity* (as defined in the first part of Section 3), it is only fair to note that the four-dimensional nature of the 1 bit/sec/Hz I-Q QPSK codes and the 3 bits/sec/Hz I-Q 16-QAM codes incur an additional encoding delay of one signaling period, relative to their conventional counterparts.
- Throughout this paper (with the lone exception of Section 3.5, below) we assume that perfect channel state information – i.e., the fading values – are available to the receiver. As noted in [25]-[28], several techniques have been proposed to recover CSI, and it is common practice in the coding literature to assume its availability (e.g., [13], [14]). However, this task is easier for constant-envelope modulation schemes (i.e., PSK) than it is for QAM-style modulation, where information is contained in both phase *and* amplitude. Thus the comparison between the 8-PSK codes from [13] and the I-Q 16-QAM codes – all 2 bits/sec/Hz – should be qualified, in that it would be more difficult to extract accurate channel state information with the 16-QAM constellation.

### 3.5 Performance Without CSI

All of the above results (as well as those in Section 4) assume that the value of the fades imposed by the channel – the *channel state information* – can be recovered perfectly; indeed,

the pairwise error bound in (4) that motivated time diversity as an important design criterion assumed the presence of perfect CSI at the receiver.

In some systems it may not be practical to attempt CSI recovery, so the question of how well I-Q TCM performs *without* CSI at the receiver becomes relevant. In the absence of CSI, the fading values are assumed to take their normalized value of one, so the decoding metric is the usual Euclidean metric:

$$m(\mathbf{y}_N, \mathbf{x}_N; \rho_N) = - \sum_{l=1}^N |y_l - x_l|^2.$$

Figure 14 shows simulation results for three different codes of the same complexity, each with a rate of 1 bit/sec/Hz operating over a channel with flat, slow Rayleigh fading.

- The worst-performing code is a conventional 16-state rate 1/2 Gray-mapped convolutional code with no CSI at the receiver.
- The next-best performing code is a 16-state I-Q QPSK code with no CSI at the receiver.
- The best of the three is the same 16-state I-Q QPSK code, this time assuming perfect CSI recovery.

From Figure 14 we see that the absence of CSI “costs” the I-Q QPSK code about 1.2 dB at a BER of  $10^{-5}$ . On the other hand, the I-Q QPSK code – which gained slightly more than 2 dB over the conventional code assuming CSI was available to each – retains that advantage over the conventional code when CSI is unavailable to each.

Finally, we note that the absence of channel state information in the higher rate codes – i.e., the 2 bits/sec/Hz I-Q 16-QAM codes and the 3 bits/sec/Hz 4D I-Q 16-QAM codes – is far more destructive. Because 16-QAM represents information with both phases and amplitudes, it is far more sensitive to fading; thus some form of CSI recovery must be used if these codes are to be implemented. Without CSI, a bit-error rate “floor” appears, making reliable communication impossible; fortunately, the work of Ho, Cavers, and Varaldi [25] has

demonstrated that practical CSI recovery with 16-QAM modulation can be effected with performance very close to that assuming perfect recovery.

## 4 Performance over Correlated Rayleigh Fading

Often, successive fading amplitudes are correlated – as in, for example, narrow-band cellular mobile radio [3]. In this section we briefly describe the performance of the proposed codes when correlated fading is assumed and appropriate interleaving is employed.

We assume the power spectral density of the faded amplitude due to Doppler shift is

$$V(f) = \begin{cases} \frac{1}{2\pi\sqrt{f_D^2 - f^2}} & \text{if } |f| < |f_D| \\ 0 & \text{otherwise} \end{cases} \quad (10)$$

Thus the autocorrelation function  $R_H(0; \Delta t)$  can be written as

$$R_H(0; \Delta t) = J_0(2\pi f_D \Delta t) \quad (11)$$

where  $J_0(x) = \sum_{n=0}^{\infty} (-1)^n \left(\frac{x^n}{2^n n!}\right)^2$  is the zero-order Bessel function of the first kind. In the simulations, the fade amplitudes are generated by applying two independent white noise sources to two filters with a spectrum shape of  $\sqrt{V(f)}$  and scaling them so that  $E(\rho_i^2) = 1$ ; an FIR filter with 200 coefficients is used to approximate the power spectrum. The filter bandwidth is specified by the vehicle speed, the carrier frequency and the symbol rate. In our simulations, we have assumed a vehicle speed of 60 mi/hr, a carrier frequency  $f_c = 900$  MHz and a symbol rate of 8000 symbols/sec. This results in a fade rate  $f_D T_s = 0.01$ .

An interleaver size of 400 symbols was used, corresponding to a delay of 50 msec. The interleaver is modeled as a buffer with  $d$  rows (depth) and  $s$  columns (span); the encoded symbols are written in successive rows and transmitted over the channel in columns. It has been shown [33] that an interleaver depth of at least one-quarter of the fade cycle provides near-optimal performance – i.e.,  $d \geq 1/(4f_D T_s)$ . For our purposes, this meant we kept the interleaver depth to at least 25 symbols; accordingly, the span  $s$  must satisfy  $s \leq 16$ .

Computer simulations were performed to determine a suitable interleaver span. Ideally, the interleaver span should be on the order of the decoder buffer size. Figure 15 shows

BER results for the 4-state I-Q 16-QAM encoded system with different decoder buffer sizes. Note that there is (relatively) little performance degradation when a buffer of size  $4\nu$  is used, compared with the case  $8\nu$ . A similar conclusion has been observed for other codes. Simulation results for a fixed interleaver size ( $s \cdot d = 400$ ) but different values of  $d$  and  $s$  are shown in Figure 16; it is observed that  $s = 4\nu$  yields the best results.

Figure 17 shows the BER results for 8-state codes with different throughputs. For the 2 bits/sec/Hz code an interleaver of dimension  $4\nu \times d = 12 \times 33$  was used. For the other two codes – with their multiplicity of two baud per branch – the guideline of  $4\nu$  stages in the decoder buffer would suggest an interleaver with span  $s = 24$ ; however, that would imply an interleaver depth of  $d = 16$ , which is less than one-quarter of the fade cycle. As a compromise, we used a  $20 \times 20$  interleaver table for the 1 bit/sec/Hz code and the 3 bits/sec/Hz code. A loss of about 1-2 dB is observed when these results are compared with the independent Rayleigh fading results in Figures 4, 6, and 10. This loss is due to the effects of correlated fading.

## 5 Conclusions

I-Q TCM schemes with bandwidth efficiencies of 1, 2, and 3 bits/sec/Hz were presented. Computer simulations and tight upper bounds show a significant improvement in bit error rate for I-Q TCM schemes relative to conventional trellis codes over the Rayleigh fading channel; coding gains close to what is expected from the cutoff rate limits are achieved for moderately complex codes. Simulations of interleaved systems confirm that an interleaver depth of  $1/(4f_D T_s)$  yields good performance, and it has been shown that a suitable value of the interleaver span is  $4\nu$ .

## References

- [1] J. Hagenauer and E. Lutz "Forward Error Correction Coding for fading Compensation in Mobile Satellite Channels", *IEEE Journal on Selected Areas in Communications*,



- February 1987, 5(2), pp. 215-225.
- [2] C.-E. W. Sundberg and N. Seshardi, "Coded Modulations for Fading Channels: An Overview," *European Trans. on Telecommunications*, May-June 1993, pp. 309-324.
- [3] W. Jakes, *Microwave Mobile Communications*, John Wiley and Sons., 1974
- [4] J. Proakis, *Digital Communications*, Mc-Graw Hill Book Company, 1989.
- [5] G. Ungerboeck, "Channel Coding with Multilevel/Phase Signals", *IEEE Transactions on Information Theory*, January 1982, 28(1), pp.55-67.
- [6] D. Divsalar and M. Simon "Trellis Coded Modulation for 4800-9600 bits/s Transmission over a Fading Mobile Satellite Channel", *IEEE Journal on Selected Areas in Communications*, February 1987, 5(2), pp. 162-175.
- [7] D. Divsalar and M. Simon "The Design of Trellis Coded MPSK for Fading Channels : Performance Criteria", *IEEE Transactions on Communications* September 1988, 36(9), pp. 1004-1012.
- [8] D. Divsalar and M. Simon "The Design of trellis Coded MPSK for Fading Channels : Set Partitioning for Optimum Code design", *IEEE Transactions on Communications*, September 1988, 36(9), pp. 1013-1021.
- [9] J. Cavers and P. Ho "Analysis of the Error Performance of Trellis-Coded Modulations in Rayleigh-Fading Channels", *IEEE Transactions on Communications*, January 1992, 40(1), pp. 74-83.
- [10] K. Chan and A. Bateman "The Performance of Reference-Based M-ary PSK with Trellis Coded Modulation in Rayleigh Fading", *IEEE Transactions on Vehicular Technology*, May 1992, 41(2), pp. 190-198.

- [11] S. Wilson and Y. Leung "Trellis-Coded Phase Modulation on Rayleigh Channels", International Conference on Communications, 1987, pp. 739-743.
- [12] H. Jamali and T. Le-Ngoc "A New 4-State 8PSK Scheme for Fast Fading, Shadowed Mobile Radio Channels", *IEEE Transactions on Vehicular Technology*, January 1991, 40(1), pp. 216-222.
- [13] C. Schlegel and D. J. Costello, Jr. "Bandwidth Efficient Coding for Fading Channels: Code Construction and Performance Analysis", *IEEE Journal on Selected Areas in Communications*, December 1989, 7(9), pp. 1356-1368.
- [14] J. Du, and B. Vucetic, "New 16-QAM Trellis Codes for Fading Channels," *Electronics Letters*, 6th June 1991, pp. 1009-1010.
- [15] N. Seshardi and C. W. Sundberg "Multi-level Trellis Coded Modulations with Large Time Diversity for the Rayleigh Fading Channel", CISS, March 1990, pp. 853-857.
- [16] N. Seshardi and C. W. Sundberg, "Multi-level Block Coded Modulations for the Rayleigh Fading Channel", GLOBECOM, 1991, pp. 047-051.
- [17] N. Seshardi and C.-E. W. Sundberg "Multilevel Trellis Coded Modulations for The Rayleigh Fading Channel", *IEEE Transactions on Communications*. September 1993, 41(9), pp. 1300-1310.
- [18] J. Wu and S. Lin "Multilevel Trellis MPSK Modulation Codes for the Rayleigh Fading Channel", *IEEE Transactions on Communications*, September 1993, 41(9), pp. 1311-1318.
- [19] E. Zehavi, "8-PSK Trellis Codes for a Rayleigh Channel", *IEEE Transactions on Communications*, May 1992, 40(5), pp. 873-884.
- [20] L.-F. Wei, "Coded M-DPSK with Built-in Time Diversity for Fading Channels," *IEEE Transactions on Information Theory*, Nov. 1993, 39(6), pp.1820-1839.

- [21] E. Leonardo L. Zheng and B. Vucetic, "Multidimensional MPSK Trellis Codes for Fading Channels," submitted to *IEEE Transactions on Information Theory*, 1994.
- [22] A. Viterbi, E. Zehavi, J. K. Wolf and R. Padovani, "A Pragmatic Approach to Trellis Coded Modulation", *IEEE Communications Magazine*, 27(7) July, 1989, pp. 11-19.
- [23] C. Heegard, S. Lery and W. Paik, "Practical coding for QAM transmission of HDTV", *IEEE Journal on Selected Areas in Communications*, 11(1), January 1993, pp. 111-118.
- [24] M. L. Moher and J. H. Lodge "TCMP-A Modulation and Coding Strategy for Rician Fading Channels", *IEEE Journal on Selected Areas in Communications*, December 1989, 7(9), pp. 1347-1355.
- [25] P. K. Ho, J. K. Cavers and J.L. Varaldi, "The Effects of Constellation Density on Trellis-Coded Modulation on Fading Channels," *IEEE Transactions on Vehicular Technology*, August 1993, 42(3), pp.318-325.
- [26] A. Bateman, "Feedforward Transparent Tone-in-band L its Implementations and Applications," *IEEE Transactions on Vehicular Technology*, August 1990, 39(3), pp.235-243.
- [27] S. Sampei and T. Sunaga, "Rayleigh Fading Compensation for QAM in Land Mobile Radio Communications," *IEEE Transactions on Vehicular Technology*, May 1993, 42(2), pp.137-147
- [28] J. K. Cavers, "An Analysis of Pilot Symbol Assisted Modulation for Rayleigh Fading Channels," *IEEE Transactions on Vehicular technology*, November 1991, 40(4), pp. 686-693.
- [29] E. Biglieri, D. Divsalar, P. Mclane and M. Simon, Introduction to Trellis-Coded Modulation with Applications. Macmillan Publishing company, 1991.
- [30] E. Zehavi and J. K. Wolf, "On the Performance Evaluation of Trellis Codes," *IEEE Transactions on Information Theory*, March 1987, 33(3), pp. 196-201.

- [31] H. Jamali, and T. Le-Ngoc, Coded-Modulation Techniques for Fading Channels, Kluwer Academic Publishers, Boston, 1994.
- [32] S. Lin and D. J. Costello, Jr., Error Control Coding : Fundamentals and Applications Prentice-Hall, 1983
- [33] P. Ho, D. Fung, "Error Performance of Interleaved Trellis-Coded PSK Modulations in Correlated Rayleigh Fading Channels," *IEEE Transactions on Communications*, December 1992, 40(12), pp. 1800-1809.

$\nu$	$g_1(D)$	$g_2(D)$
2	$1 + D^2$	$1 + D + D^2$
3	$1 + D + D^3$	$1 + D + D^2 + D^3$
4	$1 + D^3 + D^4$	$1 + D + D^2 + D^4$
5	$1 + D + D^3 + D^5$	$1 + D^2 + D^3 + D^4 + D^5$
6	$1 + D^2 + D^3 + D^5 + D^6$	$1 + D + D^2 + D^3 + D^6$

Table 1: Generator polynomials for the rate 1/2 codes.

Code	Throughput(bits/sec/Hz)	$\nu$	Time Diversity	Complexity
QPSK-Gray	1	2	3	8
I-Q QPSK	1	2	5	8
QPSK-Gray	1	3	4	16
I-Q QPSK	1	3	6	16
QPSK-Gray	1	4	5	32
I-Q QPSK	1	4	7	32
QPSK-Gray	1	5	6	64
I-Q QPSK	1	5	8	64
QPSK-Gray	1	6	7	128
I-Q QPSK	1	6	10	128
8-PSK	2	2	2	8
I-Q 16-QAM	2	2	3	8
S/C 8-PSK	2	3	2	16
I-Q 16-QAM	2	3	4	16
S/C 8-PSK	2	4	3	32
I-Q 16-QAM	2	4	5	32
S/C 8-PSK	2	5	3	64
I-Q 16-QAM	2	5	6	64
S/C 8-PSK	2	6	4	128
I-Q 16-QAM	2	6	7	128
D/V 16-QAM	3	3	2	64/3
I-Q 16-QAM	3	3	2	32/3
D/V 16-QAM	3	4	2	128/3
I-Q 16-QAM	3	4	3	128/3

Table 2: A comparison between the proposed codes and conventional TCM schemes. Codes denoted ‘‘S/C’’ are from Schlegel/Costello [13] and codes denoted ‘‘D/V’’ are from Du/Vucetic [14].

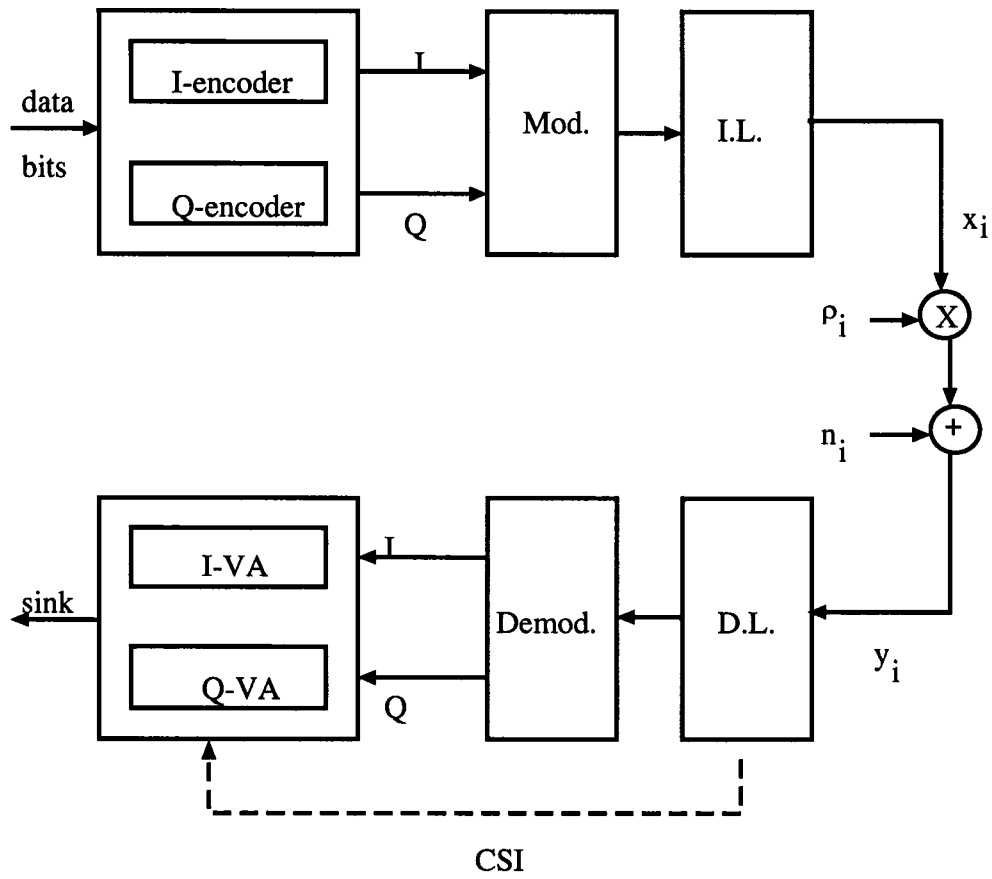


Figure 1: The structure of the proposed system.

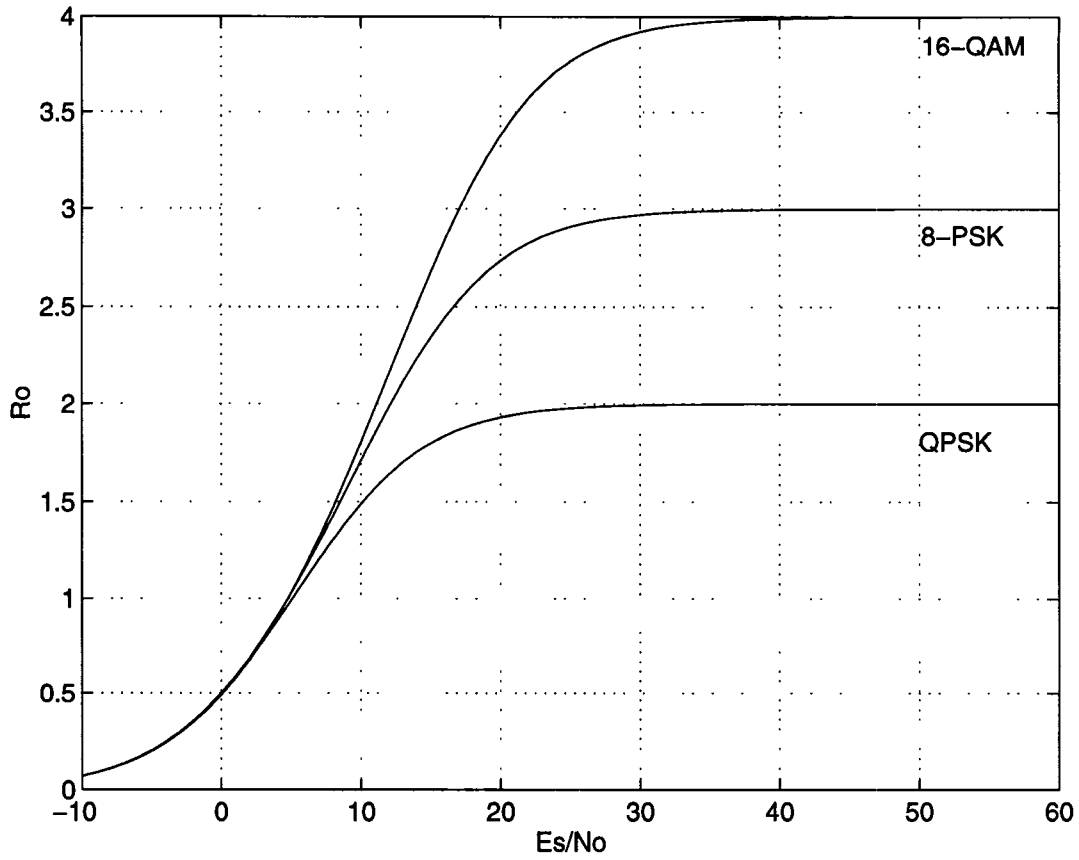


Figure 2: Cutoff rates for QPSK, 8-PSK and 16-QAM

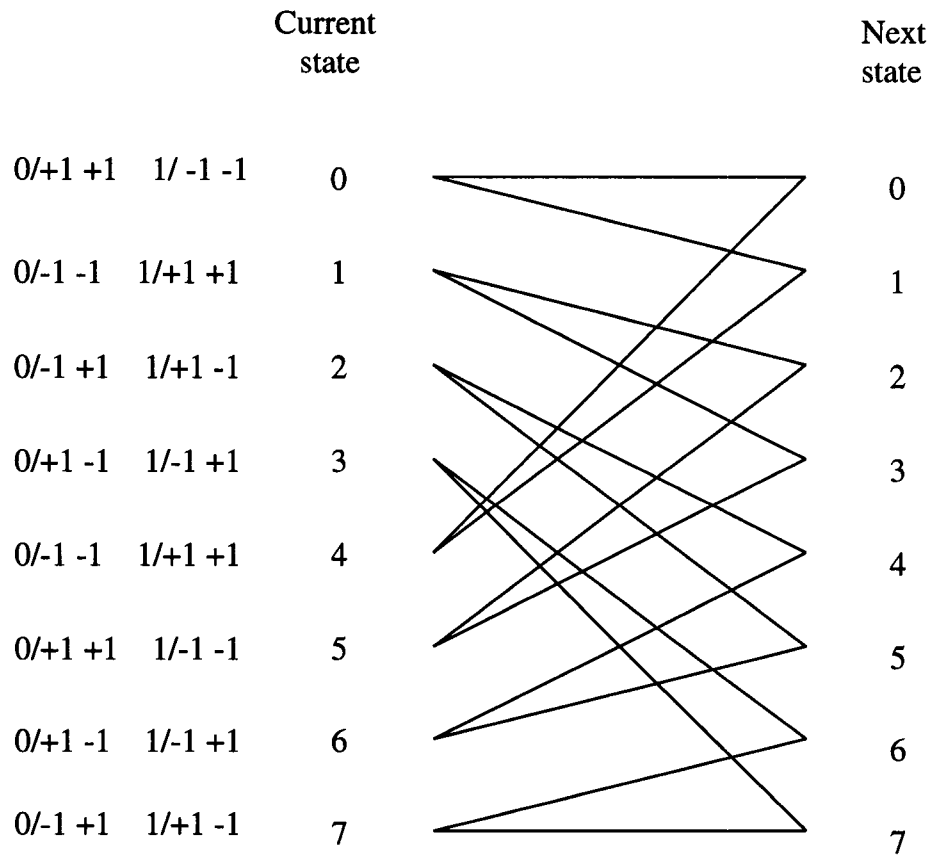


Figure 3: Trellis diagram for the 8-state I-Q QPSK code. (1 bit/sec/Hz)



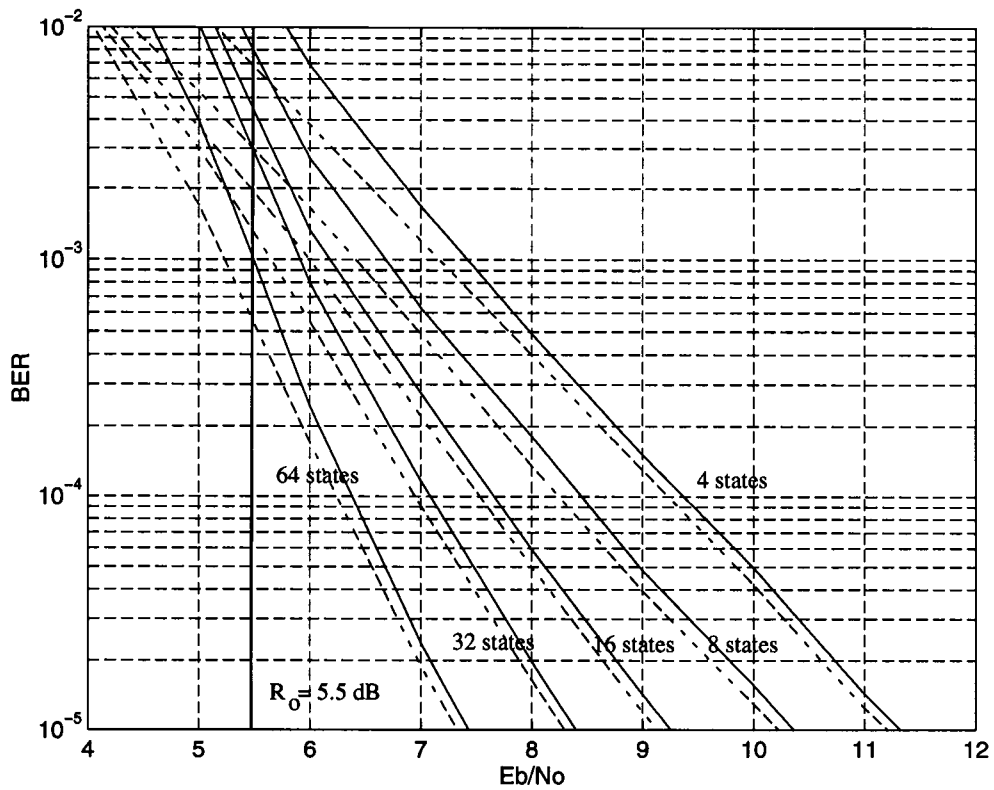


Figure 4: BER performance for 1 bit/sec/Hz I-Q QPSK. The solid lines indicate the upper bound from (6); dashed lines indicate simulation results.

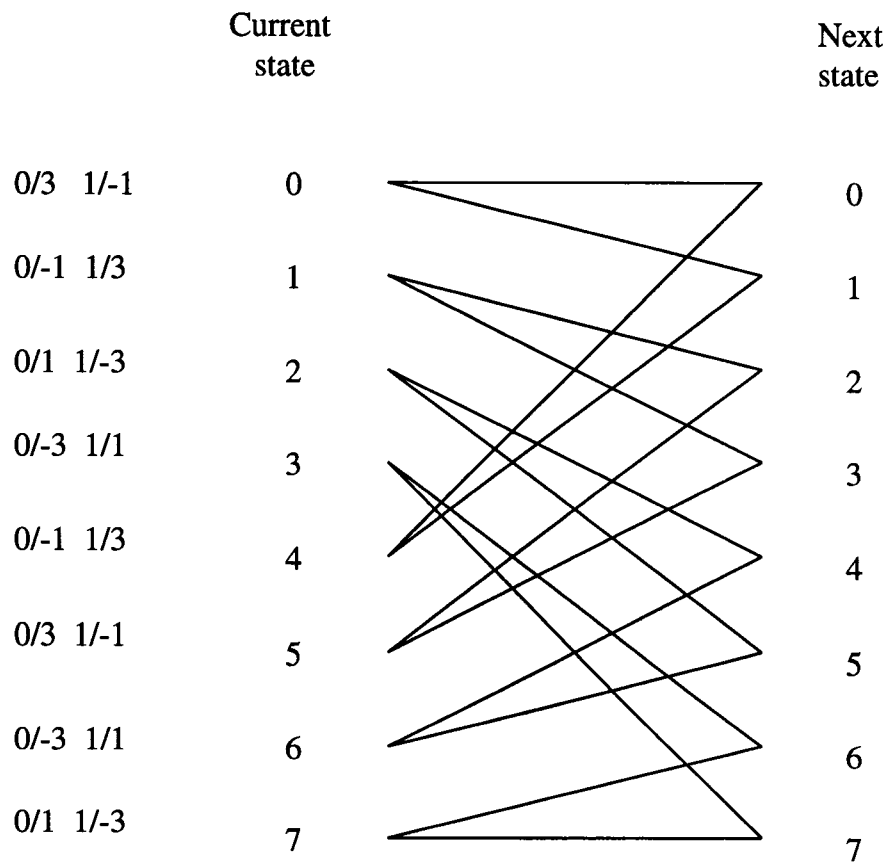


Figure 5: Trellis diagram for the 8-state I-Q 16-QAM code. (2 bits/sec/Hz)

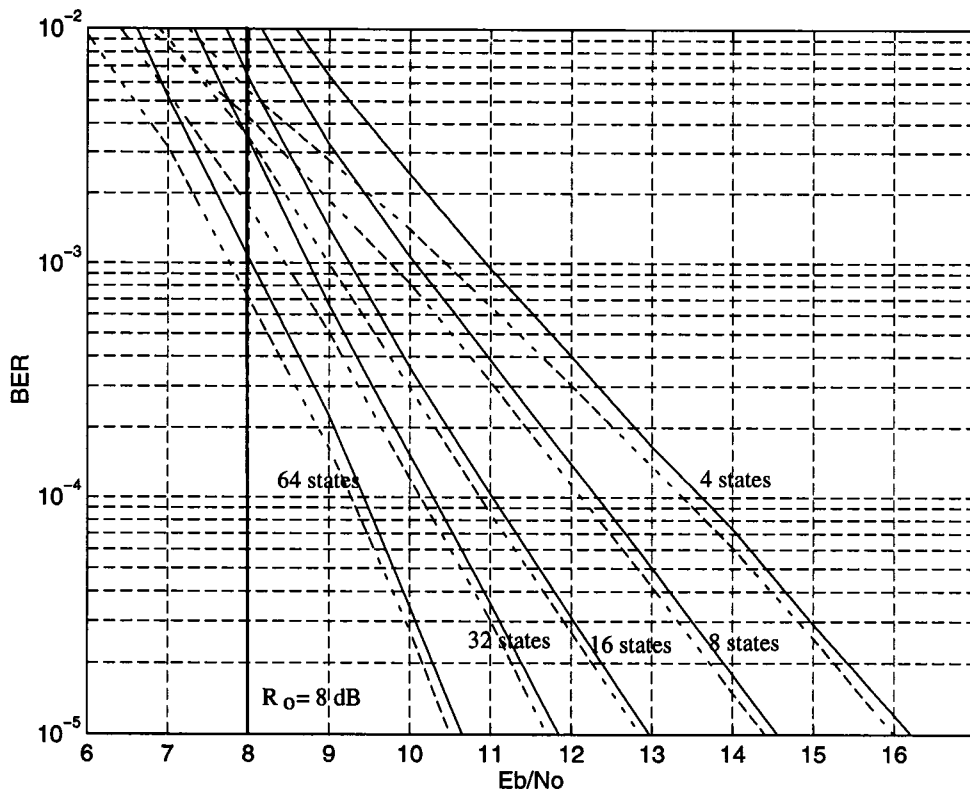


Figure 6: BER performance for 2 bits/sec/Hz I-Q 16-QAM. The solid lines indicate the upper bound from (6); dashed lines indicate simulation results.

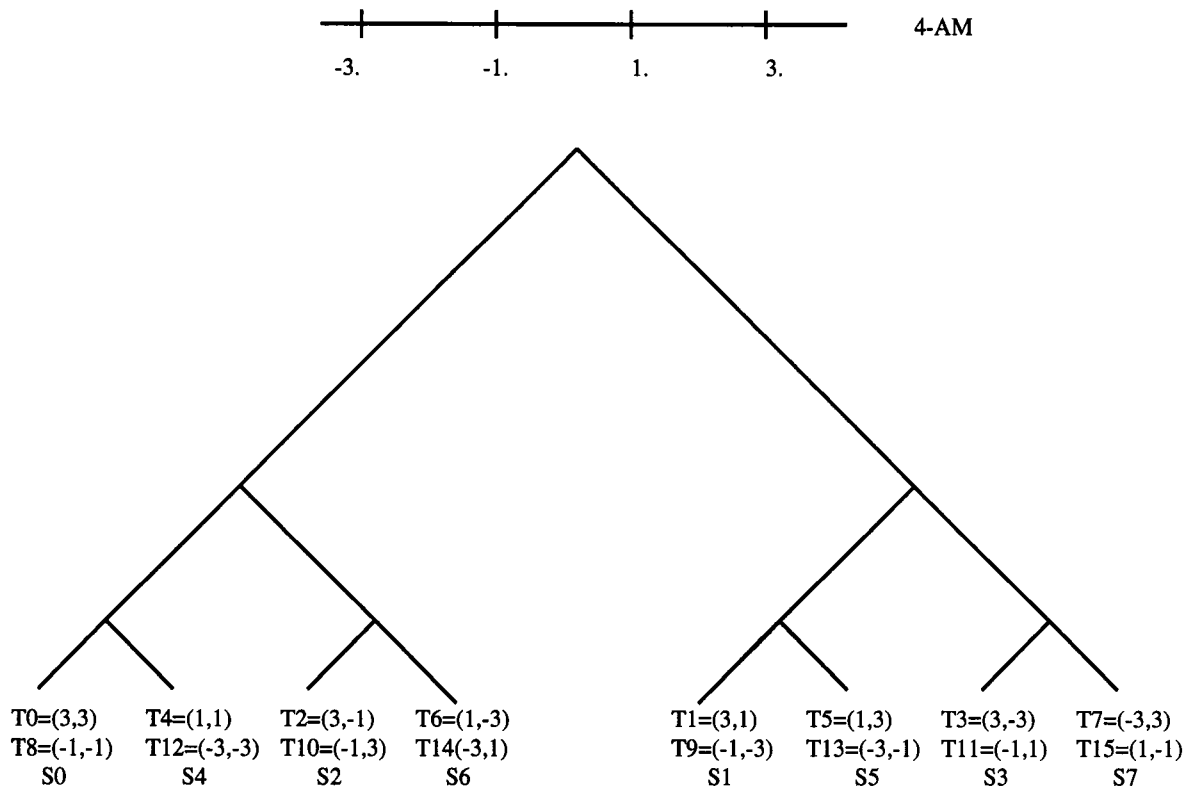


Figure 7: Signal partitioning for the 2D 4-AM constellation designed for the Rayleigh distributed channel

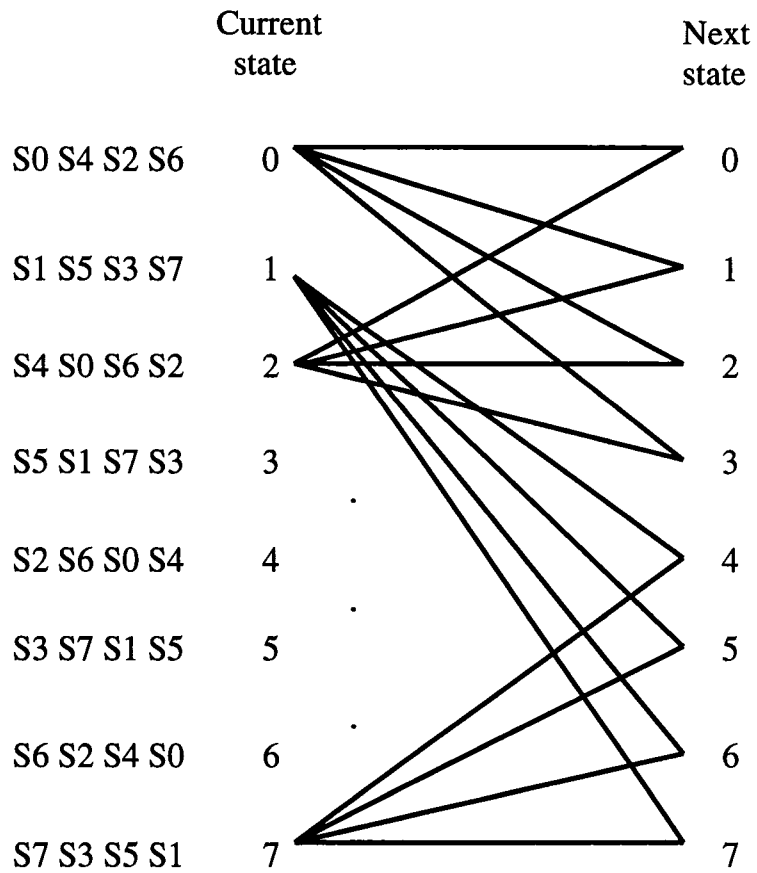


Figure 8: Trellis diagram for the 4D I-Q 16-QAM 8-state code. (3 bits/sec/Hz)

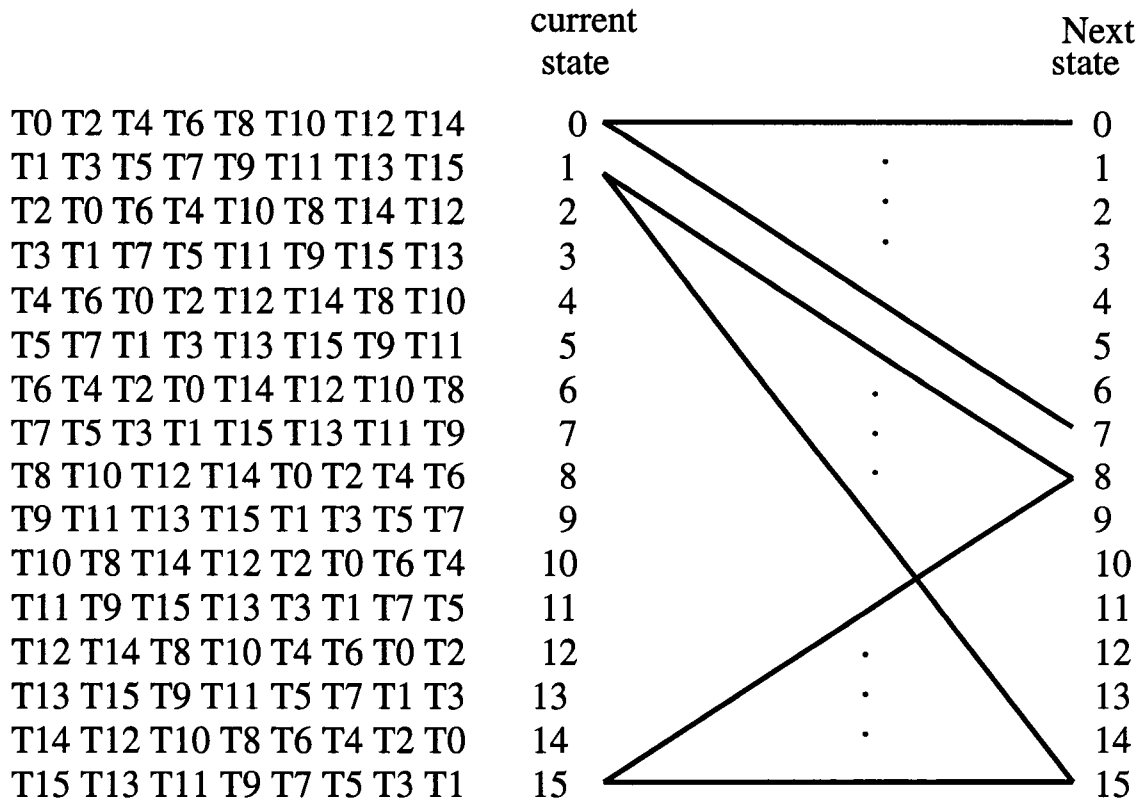


Figure 9: Trellis diagram for the 4D I-Q 16-QAM 16-state code (3 bits/s/Hz)

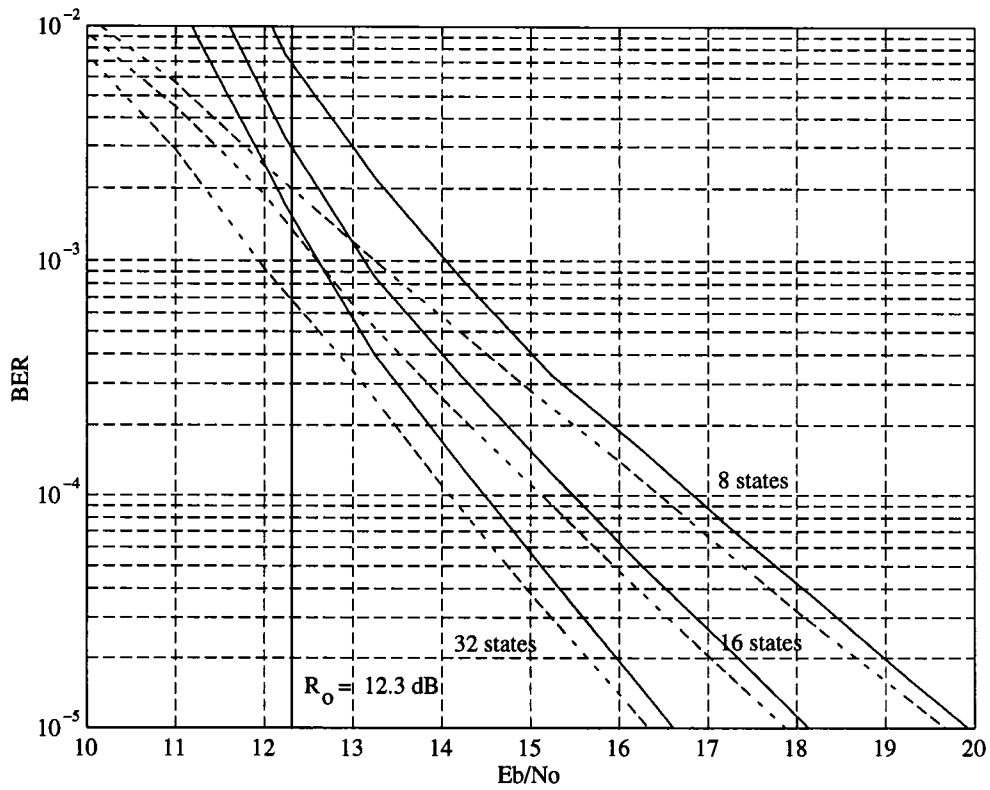


Figure 10: BER performance for 3 bits/sec/Hz I-Q 4D 16-QAM. The solid lines indicate the upper bound from (6); dashed lines indicate simulation results.

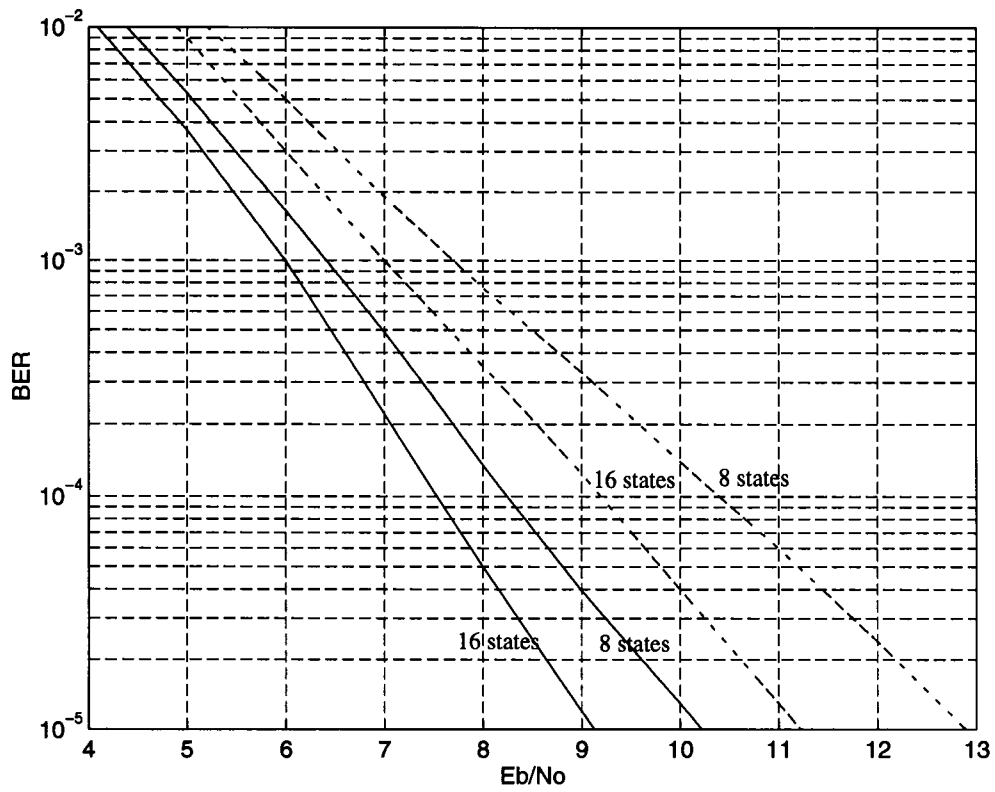


Figure 11: A comparison between the proposed 1 bit/sec/Hz code and Gray-mapped rate 1/2 convolutional coding. The solid lines indicate I-Q TCM; dashed lines indicate Gray-mapped convolutional codes.



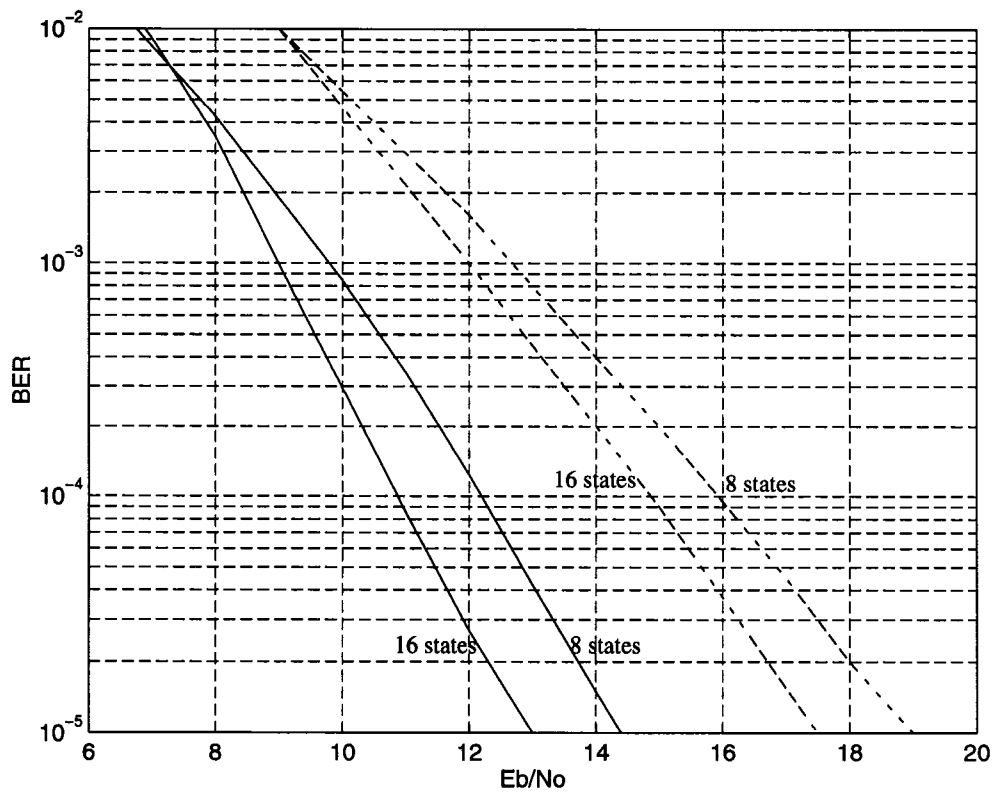


Figure 12: A comparison between the proposed 2 bit/sec/Hz code and codes from [13]. The solid lines indicate I-Q TCM; dashed lines indicate [13].

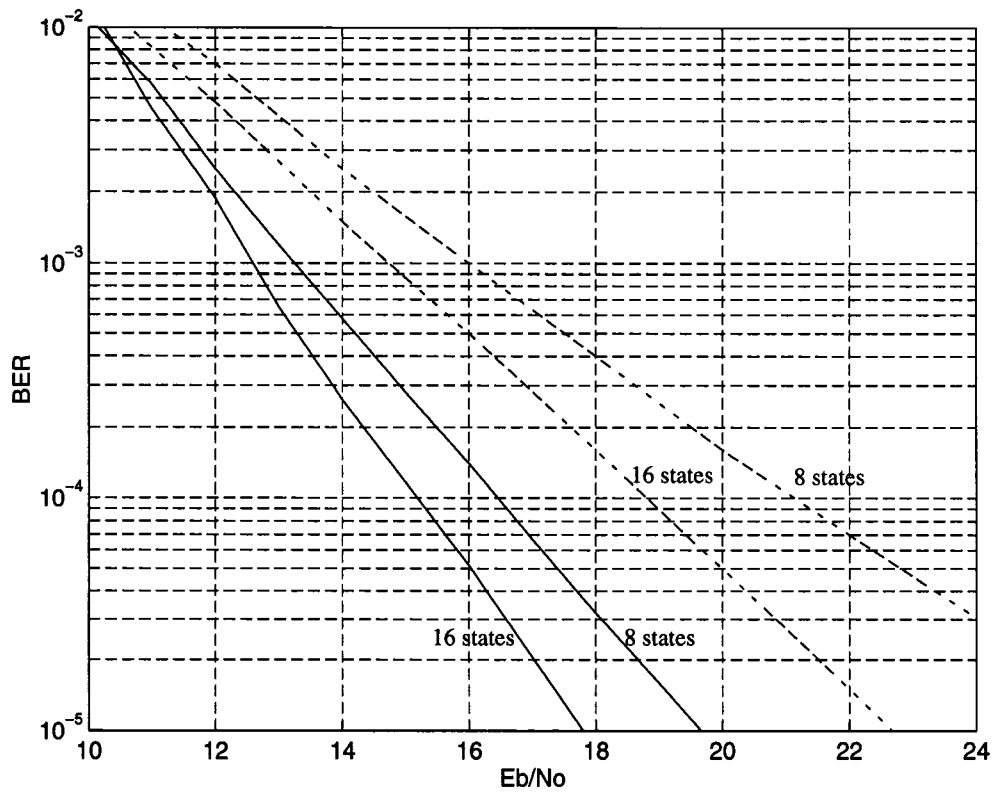


Figure 13: A comparison between the proposed 3 bit/sec/Hz code and codes from [14]. The solid lines indicate I-Q TCM; dashed lines indicate [14].

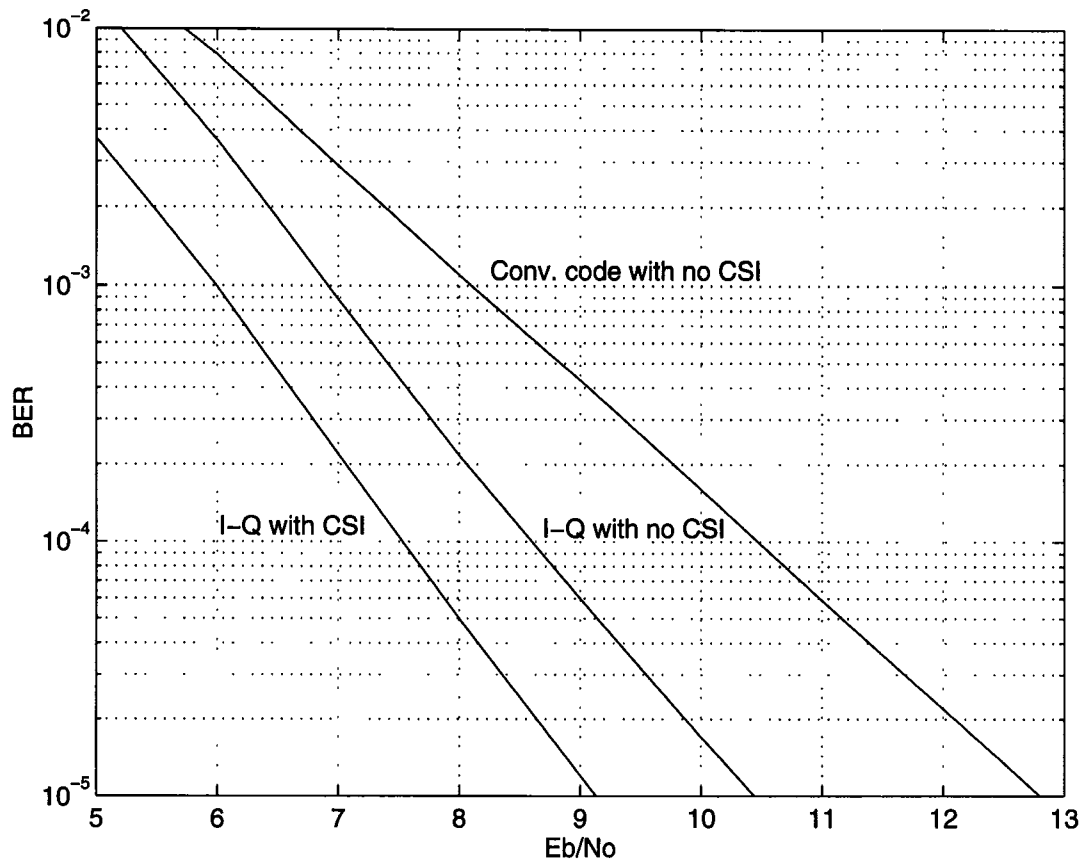


Figure 14: A comparison between Gray-mapped rate 1/2 convolutionally encoded QPSK with no CSI, I-Q QPSK with no CSI, and I-Q QPSK with CSI.

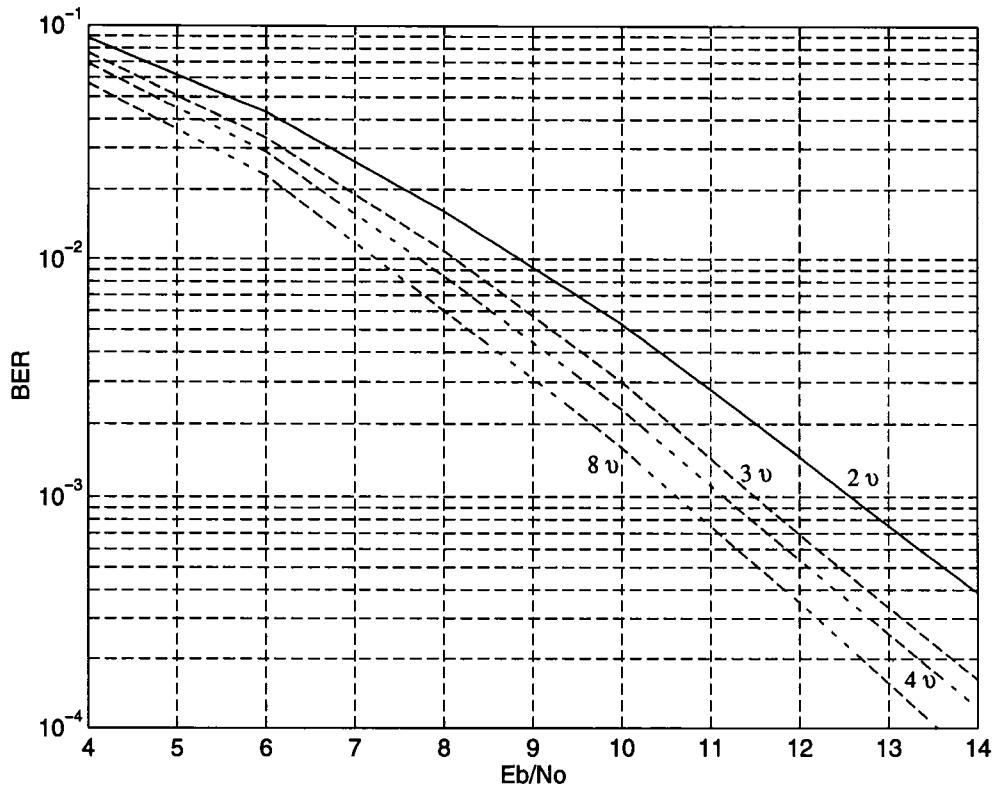


Figure 15: BER for the 4-state I-Q 16-QAM encoded system with different decoder buffer sizes.

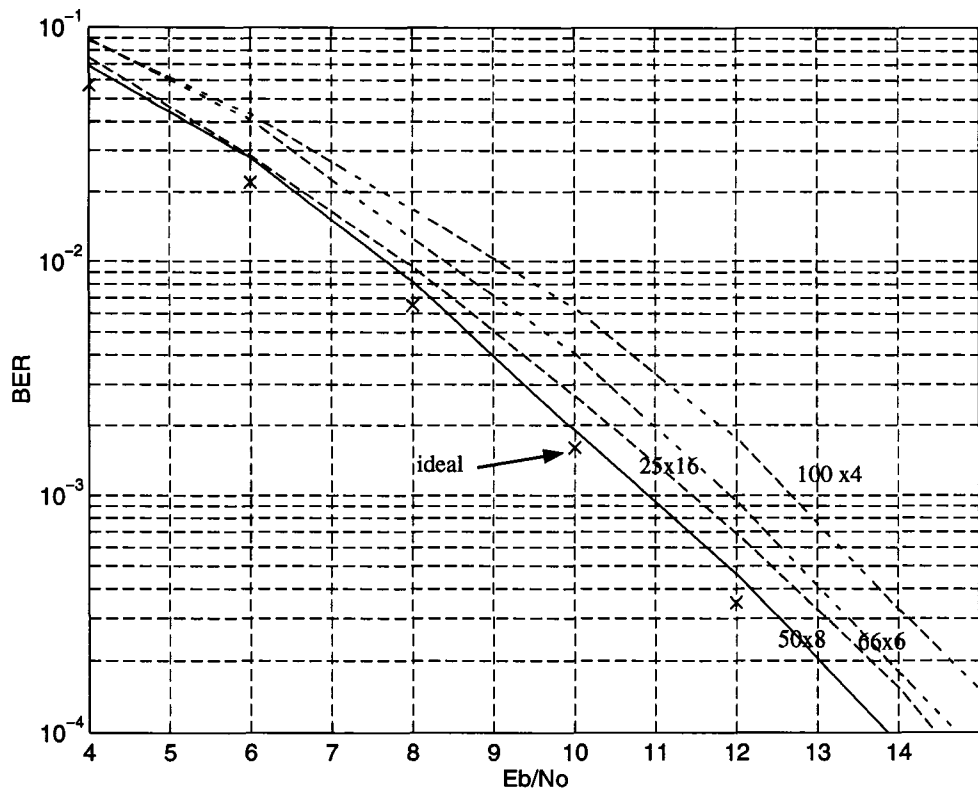


Figure 16: BER for the 4-state encoded I-Q 16-QAM with different interleaver dimensions.

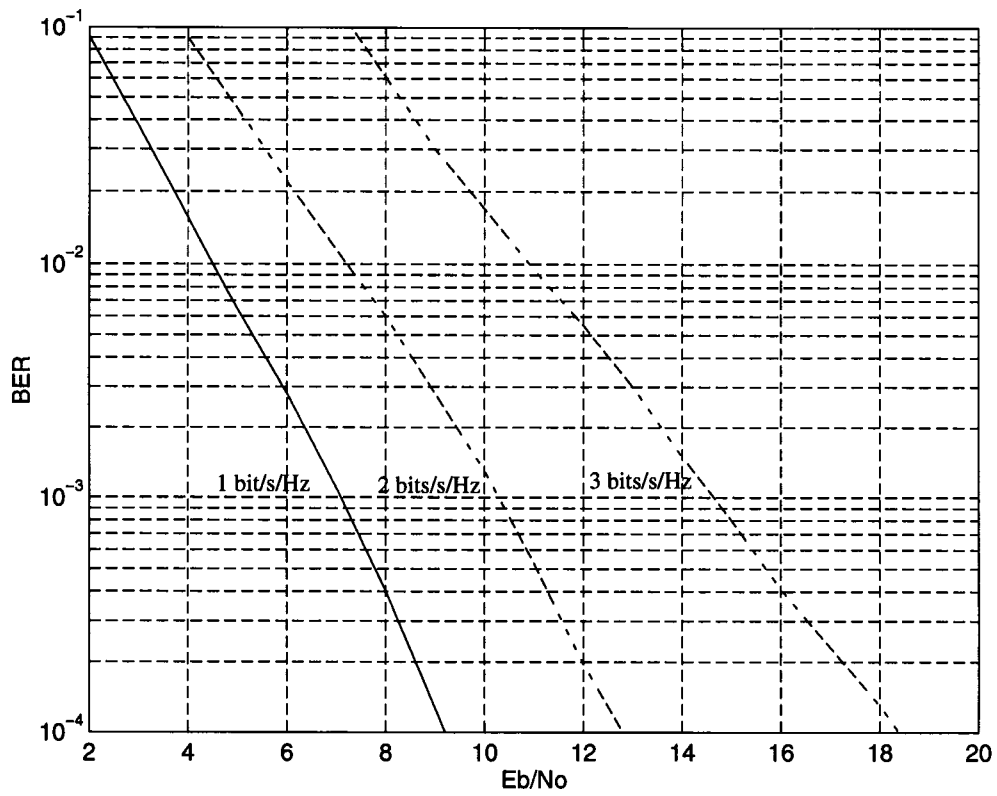


Figure 17: BER for the interleaved 8-state encoded systems with different throughputs.